Machine learning informs mitigation strategies for nitrous oxide emissions from wastewater operations

Gnanaraj Augustine, Kartik Chandran*

*Department of Environmental Engineering, Columbia University, New York, 10027, USA

ABSTRACT: This study focused on the development of machine-learning- (ML) based strategies for mitigating nitrous oxide (N_2O) emissions from various wastewater treatment systems in the United States measured using a benchmark USEPA-endorsed protocol. Results revealed that in general, poor process performance correlated with higher N_2O emissions. Specifically, local variables including zone-specific dissolved oxygen, ammonia, and nitrite concentrations and global variables including effluent nitrite and nitrate concentrations contributed positively towards N_2O emissions from both aerobic and anoxic zones of the process bioreactors. The optimal operational conditions identified for minimizing N_2O emissions included operation of aerobic and anoxic zones at DO < 4 mg O_2 L^{-1} and < 1 mg O_2 L^{-1}, respectively, coupled with appropriate solids retention times (SRTs) that maximize process performance. Accordingly, our results strongly underscore the utility of ML models in combination with bioprocess fundamentals for predicting and mitigating N_2O emissions, while concomitantly optimizing wastewater treatment operations.

KEYWORDS: *nitrous oxide, activated sludge, greenhouse gas, machine learning*

Introduction

Nitrous oxide (N_2O) is a potent greenhouse gas (GHG) and ozone depleting substance [1,2]. Wastewater treatment plants (WWTPs) have been increasingly recognized as substantial anthropogenic sources of N_2O emissions[3–7]. On one hand, increasingly stringent effluent nitrogen limits from wastewater treatment plants have spurred a global effort to develop and implement engineered biological nutrient removal (BNR) processes to improve water quality[4]. On the other hand, suboptimal operating conditions and process configurations associated with BNR operations can exacerbate N_2O production[8].

During typical WWTP nitrification operations, chemolithoautotrophic ammonia-oxidizing bacteria (AOB) and nitrite-oxidizing bacteria (NOB) sequentially oxidize ammonia (NH_3) to nitrite (NO_2^-) and nitrate (NO_3^-), respectively, using oxygen as the preferred terminal electron acceptor[9]. During denitrification, NO_3^- is reduced to dinitrogen (N_2) gas, coupled with the utilization of organic or inorganic electron donors[9]. In nitrifying WWTPs, AOB produce nitric oxide (NO) and N_2O via nitrifier denitrification under limiting dissolved oxygen (DO) and non-limiting NO_2^- concentrations[6,10–15]. Also, under non-limiting DO and NH_3 concentrations, AOB produce N_2O during the oxidation of hydroxylamine (NH_2OH) [10,16]. N_2O can also be produced through chemical oxidation of NH_2OH[10,16]. During typical engineered denitrification, chemoorganoheterotrophic bacteria produce N_2O under operating conditions that favor inhibition of nitrous oxide reductase (Nos) [16], for instance, associated with inhibition by oxygen and NO_2^-[12,17,18]. Despite the contribution of both nitrification and denitrification in N_2O production, it has now been established that both *production* and *emission* of N_2O from aerated zones are higher than from non-aerated zones at WWTPs[4].

The characterization and minimization of N_2O emissions from WWTPs has assumed widespread and critical importance as wastewater utilities aim to minimize the overall carbon footprint of treatment operations, while adhering to increasingly stringent discharge regulations[19]. Previous N_2O footprinting studies performed at full-scale BNR and non-BNR WWTPs around the United States reported N_2O emission factors (EFs) in the range 0.01-1.8% relative to the influent TKN load[4]. Other full-scale studies have reported widely varying EFs in the range 0.001-25.4% of the influent load[4,20].

N_2O production is directly correlated with nitrogen conversion dynamics in WWTPs, further indicating the potential of N_2O emissions as BNR performance indicators[4–6,20]. Various operational and environmental factors such as solids retention time (SRT),

specific AOB activity, temperature, and influent loading patterns, contribute to both N_2O emissions and overall process performance in BNR systems[4–7,20]. BNR operations at sub-optimal conditions, such as excessively high or low DO concentrations combined with inadequate SRT, can lead to transient or permanent NH_3 or NO_2^- accumulation. Such accumulation is symptomatic of inadequate nitrification and denitrification performance and can be correlated, in turn, to NO and N_2O production and emission[5–10]. Mechanistic models have been used to predict and reduce N_2O emissions in the BNR systems from WWTPs, ranging from models based on the activated sludge framework[21] to models based on gene- and protein-expression[15,22–25]. Other data-driven models have also been proposed, which when trained on robust and representative datasets, offer a balance between the mathematical and metabolic intricacies relating to N_2O production and their practical end-application for process control[4,26]. Data-driven models such as unsupervised Principal Component Analysis (PCA) and supervised machine learning (ML) models have shown greater insights into improving process performance and identifying factors contributing to N_2O emissions[27–32]. Supervised ML models have demonstrated the potential for predicting N_2O emissions from full-scale BNR operations, and studies have shown the usage of ML models focused on predicting effluent water quality[32–36] or primarily N_2O emissions.[37–40], using different models and approaches such as hyperparameter optimization (HPO)[40].

In this study, we subjected both historical and currently obtained datasets to unsupervised PCA and supervised ML modeling approaches to uncover the complex interplay between operational strategies, N_2O emissions and effluent water quality, and to develop actionable insights into WWTP operating strategies that minimize both *gaseous* and *aqueous* nitrogenous discharges. Through this research, we offer new insights into concurrently

maximizing BNR process efficiency and achieving decarbonization of BNR operations, thereby promoting a more sustainable wastewater sector.

Results

Updated N_2O emissions from advanced mainstream and sidestream activated sludge processes

We first present the results obtained from recently conducted (2023-2024) N_2O measurement campaigns at five different next-generation mainstream and sidestream wastewater treatment processes in the Northeastern and Mid-Atlantic regions of the United States (**Table 1**). For the *mainstream processes* tested, the average EF, representing the fraction of the influent nitrogen load emitted as N_2O, was statistically lower than the IPCC EF (1.6±1.2%) ($p=0.03$, $\alpha=0.05$)[3]. Within the mainstream processes evaluated, the EF for the four-pass step-feed BNR process tested (0.20±0.03%) was statistically higher ($p=0.01$, $\alpha=0.05$) than for the processes based on ammonia-based aeration control (ABAC) (0.004±0.00%), partial denitratation-anammox (PdNA) (0.006±0.00%), and fermentate-fed denitrification (0.003±0.00%). Based on these results by themselves, the mainstream processes sampled herein displayed lower EFs and improved N-removal relative to those previously characterized (**Table 1, Figure S1**). In contrast, the *sidestream process* exhibited EFs in the range 8.0±3.4 %, which were statistically higher ($p<0.05$) than both the mainstream- and IPCC-EFs.

However, some process-specific nuances could also be inferred based on the current datasets. For the mainstream PdNA process, operating temperature did not statistically impact either the BNR performance (% TN removal, which averaged 72±9 % across temperatures) or the N_2O EF (**Table 1**). In contrast, the emissions from the step-feed BNR process were higher during the lower temperature monitoring campaign (**Table 1**). On the

other hand, ABAC-based process represents distinct operating characteristics with uncoupled organic carbon, nitrification, and post-denitrification, and displayed a low EF. A specific overall N-removal efficiency for the ABAC process could not be correlated with the measured N_2O emissions, which were restricted to the aerated zones in the process (**Table 1**). Therefore, N_2O emissions are reflective of overall process operations specific to the designed process configuration and are not strictly influenced by operating temperatures alone.

The single reactor system for high activity ammonium removal over nitrite (SHARON) process tested treats post-anaerobic digestion centrate and operates via a combination of nitritation (oxidation of influent NH_3 to NO_2^-) followed by glycerol-mediated denitritation (reduction of NO_2^- to N_2). The SHARON process displayed low ammonia conversion (50.3±11.3%) and low nitrogen removal (37±16%)(**Table 1)**. These observed process performance measures corresponded with a higher N_2O EF (8.0±3.4%), relative to the other processes tested **(Table 1)**. Based on previous results, sidestream treatment processes, including those operating in partial nitritation mode can display EFs as low as 0.5%[4,41], suggesting considerable room for reduction in emissions with concomitant performance improvements in the system tested herein.

Such findings reinforce the previously demonstrated parallels between process performance and N_2O emissions from WWTPs[7,41–43]. Nevertheless, a robust approach capable of unraveling the complex interplay between process configurations, operating conditions, process performance and corresponding emissions is needed to explore the development of process optimization and decarbonization strategies and is described next.

Unraveling the Interdependencies of N_2O Flux and Process Parameters Using a Multi-Decadal Wastewater Treatment Operations Dataset

Advanced unsupervised and supervised machine learning models were employed using our present and past wastewater process operational data spanning more than a decade of process monitoring (**Table 1**), with the goal of improving both *aqueous* and *gaseous* nitrogen discharges.

First, using unsupervised principal component analysis (PCA), we revealed the interdependencies between nitrification and denitrification process variables (nitrogen species, organic compounds, suspended solids), operating conditions (SRT, influent flow rate), and measured N_2O fluxes. In the presented PCA biplots (**Figures 1A and 1B),** the length of the arrow represents the magnitude of the variable contribution. Positively correlated variables are clustered on the same side of the axis of a reference variable (for instance, N_2O fluxes), while the negative and uncorrelated variables are positioned opposite and perpendicular, respectively. We further classified the different influential factors into two categories. Specifically, zone-specific variables including NH_3, DO, NO_2^- and SRT were classified as *local variables*, since they reflect spatially discrete sampling locations within the WWTP process bioreactors. Influent and effluent water quality parameters, influent flowrate, and temperature were considered as *global variables*.

PCA-based interpretation of aerated zone emissions. Based on aerated zone data from current and previous sampling campaigns, PC1 and PC2 captured 35.7% and 19.1% of the variance, respectively (**Figure.1A**). Among the local variables, NH_3, DO, NO_2^- and among the global variables, influent TKN, influent ffCOD, effluent NO_2^-, effluent TSS, effluent ffCOD, and effluent tCOD were strongly and positively correlated with N_2O fluxes (**Figures 1, and S2A**). One fundamental interpretation of such correlations

149 between the local variables and observed N_2O emissions from the aerated zones points to
150 the role of nitrifier nitrification and nitrifier denitrification pathways. To summarize
151 briefly, during nitrifier-nitrification, kinetic limitations in conjunction with the presence
152 of non-limiting DO and NH_3 concentrations in aerated zones can lead to incomplete
153 NH_2OH oxidation by AOB, which results in NO and N_2O production therein[4,10,16].
154 Correspondingly, during nitrifier-denitrification, AOB produce N_2O primarily under
155 conditions that result in non-limiting NO_2^- concentrations, potentially exacerbated by
156 limiting DO and non-limiting NH_3 concentrations[4,10]. Of the global variables, high
157 influent TKN and effluent NO_2^- concentrations could indirectly correspond with higher
158 N_2O fluxes depending on SRT and the corresponding extant local variables (**Figure 1A**).
159 The observed positive correlation of measured N_2O fluxes with different effluent TSS and
160 organic carbon (ffCOD and tCOD) concentrations for a given degree of nitrification
161 cannot be interpreted in isolation and likely needs to be considered using more complex
162 models (such as the ML models considered below).

163 Negative correlations of SRT, zone-specific NO_3^-, and influent tCOD concentrations with
164 measured N_2O fluxes were also observed (**Figures 1A, and S2A**), suggesting overall that
165 conditions that promote full nitrification (higher zone-specific NO_3^- concentrations) at
166 WWTPs (higher SRTs) correspond to lower N_2O fluxes (in keeping with previous
167 results)[44]. In general, the link between lower N_2O emissions and lower influent tCOD
168 concentrations is indirect and points to increased oxygen availability for complete
169 nitrification compared to organic carbon oxidation[9].

170 Of the remaining global variables, effluent NO_2^- concentrations correlated positively with
171 aerobic N_2O fluxes, and likely represent the link between inadequate nitrogen removal
172 and higher N_2O emissions[4] (**Figures.1A and S2A**). The global variables captured by
173 both PC1 and PC2, including temperature, influent flow rate, influent TIN, influent NH_3,

influent VSS, effluent VSS, and effluent NH_3, did not statistically correlate with aerobic-zone N_2O fluxes (**Figures 1A and S2A**).

PCA-based interpretation of anoxic-zone emissions. For data obtained from all the previously and currently sampled anoxic zones, PC1 and PC2 captured 32.4% and 15.3% of the variance, respectively. Local variables including zone-specific DO and NO_2^- concentrations were positively correlated with measured N_2O fluxes (**Figures 1B, and S2B**). Notably, zone-specific DO and NO_2^- concentrations clustered closely together, emphasizing their potential significant interactive impacts on N_2O production again linked with poor process operation and incomplete denitrification, as also shown previously [4].

Global variables such as effluent NO_3^-, effluent NO_2^-, influent TKN, influent NH_3, and influent TIN concentrations exhibited a positive correlation with N_2O fluxes (**Figures 1B and S2B**). In contrast, zone-specific NO_3^- concentrations and influent flow rate were negatively correlated with N_2O fluxes (**Figure 1B**). Effluent TKN and effluent NH_3 concentrations were not statistically correlated with N_2O fluxes (**Figures 1B and S2B**).

Hyperparameter Optimization of ML Models for Predicting N_2O Flux under Different Wastewater Treatment Parameters

We further developed ML models with combinations of different process variables and parameters from our past and present data to predict and mitigate N_2O emissions from WWTP operations. The ML models were trained to predict N_2O flux (g-N/min-m^2), N_2O emission rate (g-N/d), and N_2O concentration (ppm) using three machine learning algorithms namely Random forest (RF), Gradient Boosting (GBM), and XG Boost. Each model was optimized under different hyperparameter tuning to identify the optimum parameter for achieving the best prediction performance (**Table S1**). Among these, XG boost consistently demonstrated superior performance, achieving an R^2 of 0.98 for aerobic

198 N_2O flux and 0.86 for anoxic N_2O flux prediction (**Table S2**). The Root Mean Square
199 Error (RMSE) for XG Boost was significantly lower compared to RF and GB, with values
200 of 0.69 and 0.20 for aerobic and anoxic conditions (**Table S2**).

201 **Machine Learning Insights into the Direct Impact of Wastewater Effluent Quality**
202 **on N_2O Flux**

203 From the trained ML models, permutation importance was extracted for both aerobic and
204 anoxic zone conditions (**Figure 2A-C**). Of the 24 variables trained (**Figure S3**), only the
205 top fiveteen are showed in **Figure 2B,C**. The most important variables contributing to
206 aerated-zone N_2O emission fluxes included influent flow rate, local NH_3, DO, and NO_2^-
207 concentrations, SRT, effluent NO_2^-, effluent NO_3^-concentrations, effluent tCOD, effluent
208 ffCOD, and effluent TSS (**Figure 2B**). For non-aerated zones, the most important
209 variables contributing to N_2O emission fluxes were zone-specific DO, NO_2^- and NO_3^-
210 concentrations, SRT, effluent NO_3^-, effluent tCOD, effluent ffCOD, effluent VSS, and
211 effluent TIN concentrations **(Figure 2C)**. These variables identified by the ML models as
212 influential predictors of N_2O fluxes were consistent with the PCA analysis and
213 underscored the now well-established link between process performance and emissions[4].
214 Our results also aligned with findings from a similar ML study using AdaBoost, which
215 pointed to temperature, DO, NH_3, NO_2^-, and NO_3^- as being influential factors for aerobic
216 zone N_2O emissions, without corresponding insights into anoxic-zone emissions[27]. Our
217 study additionally highlights the critical need to consider quantifying and predicting N_2O
218 emissions from anoxic zones, as their contribution to N_2O production and emissions are
219 inevitably under poor operating conditions[4,5].

220 We further integrated SHapley Additive exPlanations (SHAP) analysis to uncover the
221 magnitude and directionality influence of the variables towards predicted N_2O flux,

222 bridging the gap between model predictions and actionable process insights. *SHAP*
223 *analysis for aerobic* N_2O flux indicates that influent flow rate is the most significant
224 variable compared to others (**Figure 3A**). An increase in influent flow rate positively
225 influences higher N_2O flux, as it is on the positive side of the SHAP values. NH_3 and DO
226 demonstrate considerable influence as elevated NH_3 SHAP value and its concentrations
227 explain increased N_2O flux, while higher DO levels can result in both higher and lower
228 N_2O flux, depending on the condition. The results show that operation under non-limiting
229 NH_3 concentrations can lead to N_2O production, regardless of whether DO levels are high
230 or low. Therefore, optimizing DO levels *in conjunction with* appropriate NH_3
231 concentrations is essential for effective nitrification.

232 Our results also suggest potential interactive effects of operating SRT with DO and NH_3
233 concentrations (**Figure 3A**), which has a firm biochemical basis. For instance, operation
234 at elevated SRT can lead to reduced N_2O fluxes, when coupled with optimization of DO
235 concentrations to achieve a given NH_3 conversion. Based on our data, NO_2^-
236 concentrations had a lower impact on N_2O fluxes compared to that of NH_3, DO, and SRT.
237 Again, the production of NO_2^- can only be controlled by concurrently optimizing DO and
238 SRT along with NH_3 concentration.

239 Based on *SHAP analysis for anoxic* zones, the N_2O fluxes therein were highly influenced
240 by DO concentrations (**Figure 3B**), which could be linked to DO-mediated inhibition of
241 N_2O reduction to N_2[4,5,18]. A biphasic response of N_2O fluxes to SRT values was observed
242 once again pointing to possible interactions with extant DO and NO_2^- concentrations.
243 NO_3^- on the other hand, influenced anoxic-zone N_2O to a lower extent. Higher NO_3^-
244 feature value representing higher SHAP value (**Figure 3B**) does not directly imply its
245 involvement in producing N_2O. The global variables, effluent NO_2^- and NO_3^- have higher
246 feature values in the positive side of the SHAP for both aerobic and anoxic zones (**Figure**

247 **3A,B**), reflecting that higher effluent NO_2^- and NO_3^- correlate with increased N_2O flux as
248 it represents an incomplete nitrification and ineffective denitrification process. In addition,
249 SHAP analysis for N_2O emission rate and N_2O concentration under both aerobic and
250 anoxic zones are provided in **Figure S4,** further supporting these trends.

251 **Optimization of Process Performance from the ML Predictive Outcome**

252 ***i.Aerobic zone optimization***

253 The process optimization approach entailed identifying operating ranges for SRT, which
254 is the principal process parameter coupled with process performance responses that
255 concurrently minimize off-gas N_2O fluxes, via PDP analysis. **Figure 4A** suggests that
256 NH_3 concentrations < 3 mg L^{-1} at a SRT < 10 days show less N_2O flux. To study the
257 relationship between DO and NH_3, **Figure 4B** suggests that operating conditions that
258 achieve NH_3 concentrations < 3 mg L^{-1}, with DO concentration < 4 mg O_2 L^{-1}, are effective
259 in minimizing N_2O production. In contrast, operating conditions that foster concomitant
260 non-limiting DO and NH_3 concentrations, correspond to high N_2O fluxes **(Figure 4B).**
261 Such predictions are in excellent alignment with fundamental and mechanistic
262 understanding of drivers for N_2O emissions under aerobic conditions at WWTPs, via a
263 combination of oxidative and reductive pathways primarily in AOB[4–9,41–45].

264 ***ii.Anoxic zone optimization***

265 Similarly, conditions that minimize N_2O fluxes from anoxic zones included operation at
266 DO concentrations < 1 mg O_2 L^{-1}, coupled with a total process SRT < 20 days (**Figure**
267 **4C)**. Higher N_2O emissions observed at DO concentration > 1 mg O_2 L^{-1}, at SRT < 20
268 days (**Figure 4C**), also corresponded with NO_2^- accumulation in the anoxic zone (**Figure**
269 **4D)**. However, non-limiting DO and NO_2^- concentrations promote high N_2O flux despite
270 operation at SRTs > 20 days (**Figures 4C-D**). In a more general sense, we acknowledge

that operation at such high SRT values may not be an option for typical WWTPs that employ suspended-phase activated sludge processes. Therefore, the most potent primary lever for anoxic zone optimization remains appropriate DO control to minimize both NO_2^- accumulation and N_2O emission therein, while maximizing denitrification performance. Where and when possible, the ability to operate at high SRTs could provide secondary relief against sub-optimal operation and emissions.

Discussion

Poor process operation leads to high N_2O emissions irrespective of process configuration and temperature variations.

Based on a combination of current measurements and extensive historical datasets, we determined that less than optimal process operations can manifest themselves in combinations of both local and global variables that in turn are correlated with higher N_2O production and emission across aerobic and anoxic zones. Among the identified variables, SRT and DO emerged as the critical control factors governing emissions. The key local and global variables identified from the unsupervised PCA followed by supervised ML permutation importance and SHAP align well with the established understanding of the nitrification and denitrification processes[4–7,29–31], thus providing consistent insights into the contribution and significance linking to the process operation, N_2O emission, and effluent water quality. The PDP analysis conducted for aerobic zones illustrates the relationship of NH_3 concentration with key process control variables, DO and SRT, identifying the optimal operating conditions for effective nitrification and reduced N_2O flux (**Figure 4A, B**). Similarly, in anoxic zones, the PDP analysis highlights the interactions among DO, SRT, and NO_2^- pinpointing optimal conditions to achieve effective denitrification and reduced N_2O emissions (**Figure 4C,D**). The findings from

ML-based analysis reveal the interplay between the operational variables and their dynamic environment, that contribute to N_2O fluxes. Nevertheless, such analyses need to integrate fundamental biochemical understanding, to provide appropriate real-time WWTP optimization strategies that minimize both *aqueous* and *gaseous* nitrogenous discharges.

Integration of real-time process control based on ML framework

This study positively demonstrates the potential of data-driven models for process control and optimization. Upon further integrating such models into Supervisory Control And Data Acquisition (SCADA) systems, they continuously process data generated from real-time or non-real-time measurements, facilitating the development of digital twin architectures based on model-based systems engineering (MBSE)[46]. Data-driven models can provide early fault detection, and advanced process control capabilities, which mechanistic models typically cannot deliver using real-time data[46]. Indeed, previous studies have successfully applied data-driven approaches in real-time reactor operations, enhancing reactor performance and effluent water quality [47–50]. The emphasis on data-driven modeling for GHG emissions, particularly N_2O emissions, continues to expand, driven by ongoing efforts to understand their process dynamics better and improve forecasting accuracy[27,37–40]. As such, substantial opportunities exist to combine the capabilities of advanced interpretation tools such as PDP, and data-driven modeling with digital and hybrid twin systems for optimizing WWTP operations, including managing their GHG footprint.

Materials and Methods

Field Data Collection using an USEPA Approved Protocol to Measure N_2O Emissions from BNR Processes

The currently reported overall N_2O measurement campaign was performed at three different BNR wastewater treatment plants around the US. **Table S3.** provides an overview of the sampling techniques performed across both mainstream and sidestream WWTPs. The gaseous N_2O emission concentrations from the BNR processes were quantified using an USEPA endorsed protocol[51]. The Surface Emission Isolated Flux Chamber (SEIFC), the only floating body approved by the Environmental Protection Agency (EPA), has a circular cross-sectional area of 0.13 m^2 and is used to measure gaseous nitrogen fluxes from activated sludge tanks[51,52]. The SEIFC was employed to obtain headspace N_2O concentration(ppm) and fluxes at distinct locations (aerated and nonaerated) in the treatment process sampled. At each location, online measurements of gaseous N_2O concentration and gas flow were conducted over a 24-hour period to address the diurnal variability of gas emissions. The gaseous N_2O concentration was measured via infrared gas filter correlation (Teledyne API, San Diego, California) at a frequency of 1/min. For emission measurements from the closed-surface, sidestream SHARON process, the N_2O analyzer was directly connected to the off-gas stacks. Mainstream N_2O measurements were conducted at both aerobic and anoxic zones in the target WWTPs. Measurement campaigns in both mainstream and sidestream processes were conducted over multiple days to determine the spatial and temporal variability. The use of GC-TCD in past studies to measure the off-gas flow has provided valuable data at different WWTPs around US[4,52]. We used a hotwire anemometer to directly measure the off-gas flow rates from the aerated and non-aerated zones, rather than relying on process blower data for

343 approximating emission rates from aerated zones alone (**Supplementary section 8,**
344 **Figures. S5-S7).**

345 Concomitantly, during each monitoring campaign, wastewater nitrogen species
346 concentrations, including influent and effluent bioreactor samples were obtained using an
347 autosampler every 1 hour to measure NH_3, NO_2^-, and NO_3^- concentrations using a Lachat
348 Quickchem Flow injection analysis system [54]. Activated sludge mixed-liquor temperature,
349 pH, DO are acquired from the SCADA system and soluble chemical oxygen (sCOD) and
350 total chemical oxygen demand (tCOD) were measured with Hach TNTplus kits and a
351 Hach DR2800 spectrophotometer (HACH Loveland, CO). Mixed-liquor suspended solids
352 (MLSS) and volatile suspended solids (VSS) concentrations were analyzed using
353 Standard Methods 2504D and 2540E [54].

354 Bioreactor profile samples were collected from nitrifying and denitrifying tanks once a
355 day to measure NH_3, NO_2^-, and NO_3^- concentrations using Hach TNTplus kits and a Hach
356 DR2800 spectrophotometer (HACH Loveland, CO). DO concentrations, temperature (℃),
357 and pH were measured using HACH handheld sensors (HACH Loveland, CO). Process
358 air flow rate (standard cubic feet per minute, SCFM), SRT, the surface area of the tanks
359 (m^2), and influent flow rates (million gallons per day, MGD) were obtained from the plant
360 operation records.

361 The N_2O fluxes were calculated from both aerated and non-aerated zones using Eq.1, and
362 the emissions were calculated using Eq.2.

363 $$N_2O_{Flux}\left(\frac{g-N}{min-m^2}\right) = \left(\frac{(V_{air}*A_t*1000*60)+Q_{N2O_inst}}{A_{SEIFC(}m^2)}\right) * C_{N_2O} \quad \textbf{Eq.1}$$

364 $$N_2O_{ER}\left(\frac{g-N}{d}\right) = N_2O_{Flux} * A_{tank} * 1440 \quad \textbf{Eq.2}$$

$$EF\ \% = \frac{N_2O_{ER}\left(g-\frac{N}{d}\right)}{\text{Influent TKN Load}\left(g-\frac{N}{d}\right)} * 100 \qquad \textbf{Eq.3}$$

Where N_2O_{flux} is the measure of N_2O flux(g-N/min.m^2) from the activated sludge tank, V_{air} is the air velocity (m.s^{-1}) measured in the anemometer from the SEIFC parallel to the N_2O concentration measurements, A_t is the Area of the tube(m^2), Q_{N2O_inst} is the off-gas flow recorded on the N_2O analyzer (L.min^{-1}) from the SEIFC, A_{SEIFC} is the area of the flux chamber (m^2) and C_{N2O} is the average concentration of the gaseous N_2O concentration (g-N.L^{-1}). N_2O_{ER} is the N_2O emission rate (g-N/d) from the overall tank, and A_{tank} is the area of the activated sludge tank (m^2). To determine the Emission Factor (EF), the Q_{N2O} (N_2O emission rate (g-N/d)) was normalized to the influent Total Kjeldahl Nitrogen (TKN) (g-N/d) load using Eq.3.

Data Preprocessing for Calculating EF and Implementing Unsupervised PCA Analysis

The measured data were first grouped into zone-specific aerobic and anoxic zone measurements to calculate N_2O emission rates and EF across the system **(Figure 2A)**. All datasets in this study were expressed to two significant figures. Past and present datasets were screened to identify missing and non-numeric values before initiating any machine learning analysis. Missing values were imputed using the *missForest* package in R, which robustly handles non-linear relationships between variables[55].

For dimensionality reduction, an unsupervised PCA analysis was conducted. The processed datasets were arranged by aerobic and anoxic zone conditions and analyzed using the *prcomp* function. PCA visualizations were developed using the *factoextra* package. Pearson correlations were computed and correlation heatmaps were generated using *corrplot* and *ggcorrplot*.

Supervised Machine Learning Approach to Predict N_2O Fluxes

Prior to model training, the response variables N_2O flux, N_2O emission rate and N_2O concentration were log-transformed using *log1p* function to handle skewness and zero values. Each log-transformed response was then min-max scaled to the [0,1] ranges based on the training set, and the same scaling was applied to the test set to avoid information leakage. The predictor dataset included influent, effluent, and process variables under both aerobic and anoxic zones, where predictor distributions exhibited strong skewness (more than 1), log-transformed versions were created and substituted into the modeling dataset. The pre-processed data were randomly partitioned into 75% training and 25% testing subsets, with the training set further divided into 10-fold cross-validation (cv) partitions using the *caret* package to guide hyperparameter optimization.

Machine Learning Models and Hyperparameter Optimization

Three ensemble tree-based supervised ML models were implemented namely Random Forest (RF), Gradient Boosting (GB), and Extreme Gradient Boosting (XG Boost). All model training and hyperparameter tuning were performed in RStudio using the *caret*, *randomForest*, *gbm,* and *xgboost* libraries.

For XG boost, a grid search strategy was employed to optimize model hyperparameters, including the number of boosting iterations, maximum tree depth, learning rate, minimum child weight, and subsample ratios (**Supplementary Section 3**). The squared-error objective was used, so tree splits were guided by reduction in squared error. The optimal parameter set was identified by maximizing mean cross-validation performance across the 10 folds, providing a robust estimate of generalization accuracy while mitigating overfitting.

Model Evaluation and Comparison

Predictive performance of the ML models was evaluated using both regression-based metrics and process-based validations. **Table S2** reports the regression-based metrics, including the coefficient of determination (R^2), which estimates the proportion of variance explained by the models. Mean Square Error (MSE) and Root Mean Square (RMSE) were also used to quantify the magnitude of prediction errors across different ranges of N_2O fluxes under both aerobic and anoxic conditions.

Residuals were computed as the difference between measured and predicted N_2O flux values. Predictions generated in the normalized and log-transformed space were subsequently back-transformed to the original scale using the *expm1* function and reverse min-max scaling. This procedure ensured that model outputs could be directly compared to measured fluxes on their native scale.

Tools for N_2O Flux Prediction and Model Interpretation

To interpret model predictions and evaluate the contributions of individual process variables to N_2O fluxes, model-agnostic permutation importance was employed for all the models trained. This approach provided a consistent and comparable measure of variable influence across models by quantifying the change in prediction error when variable was randomly permuted, thereby capturing its relative impact on model performance.

As a complementary model-agnostic method, SHAP analyses were computed using *iml* package with a custom prediction function tailored to the XG Boost model. Both instance-level and global SHAP values were extracted. Beeswarm plots were constructed using *ggbeeswarm* and scaled efficiently with *shapviz*, while the *viridis* palette was applied to encode feature values in a perceptually uniform and colorblind-friendly manner. On the other hand, PDPs were generated using the *pdp* package to capture the marginal

relationship between predictor variables and predicted N_2O fluxes in a two-dimensional scale. To improve interpretability, feature values were back-transformed from normalized space to their original measurement scales prior to visualization. Interactive PDP and SHAP outputs were developed using *plotly*, allowing dynamic explorations of variable effects on predicted N_2O fluxes.

References

1. Ravishankara, A. R., Daniel, J. S. & Portmann, R. W. Nitrous Oxide (N_20): The Dominant Ozone-Depleting Substance Emitted in the 21st Century. *Science* **326**, 123–125 (2009).
2. Stocker, T. *Climate Change 2013: The Physical Science Basis: Working Group I Contribution to the Fifth Assessment Report of the Intergovernmental Panel on Climate Change*. (Cambridge University Press, 2014).
3. 2019 Refinement to the 2006 IPCC Guidelines for National Greenhouse Gas Inventories — IPCC. https://www.ipcc.ch/report/2019-refinement-to-the-2006-ipcc-guidelines-for-national-greenhouse-gas-inventories/.
4. Ahn, J. H. *et al.* N2O emissions from activated sludge processes, 2008-2009: Results of a national monitoring survey in the united states. *Environmental Science and Technology* **44**, 4505–4511 (2010).
5. Rassamee, V., Sattayatewa, C., Pagilla, K. & Chandran, K. Effect of oxic and anoxic conditions on nitrous oxide emissions from nitrification and denitrification processes. *Biotechnology and Bioengineering* **108**, 2036–2045 (2011).
6. Yu, R., Kampschreur, M. J., Loosdrecht, M. C. M. van & Chandran, K. Mechanisms and Specific Directionality of Autotrophic Nitrous Oxide and Nitric Oxide Generation during Transient Anoxia. *Environ. Sci. Technol.* **44**, 1313–1319 (2010).
7. Brotto, A. C. *et al.* Characterization and mitigation of nitrous oxide (N2O) emissions from partial and full-nitrification BNR processes based on post-anoxic aeration control. *Biotechnology and Bioengineering* **112**, 2241–2247 (2015).

8. Kampschreur, M. J., Temmink, H., Kleerebezem, R., Jetten, M. S. M. & van Loosdrecht, M. C. M. Nitrous oxide emission during wastewater treatment. *Water Research* **43**, 4093–4103 (2009).

9. Grady, C. P. L. *Biological Wastewater Treatment*. (New York : Marcel Dekker, 1999).

10. Chandran, K., Stein, L. Y., Klotz, M. G. & Van Loosdrecht, M. C. M. Nitrous oxide production by lithotrophic ammonia-oxidizing bacteria and implications for engineered nitrogen-removal systems. *Biochemical Society Transactions* **39**, 1832–1837 (2011).

11. Zumft, W. G. Cell biology and molecular basis of denitrification. *Microbiol Mol Biol Rev* **61**, 533–616 (1997).

12. Kester, R. A., De Boer, W. & Laanbroek, H. J. Production of NO and N(inf2)O by Pure Cultures of Nitrifying and Denitrifying Bacteria during Changes in Aeration. *Appl Environ Microbiol* **63**, 3872–3877 (1997).

13. Ritchie, G. A. & Nicholas, D. J. Identification of the sources of nitrous oxide produced by oxidative and reductive processes in Nitrosomonas europaea. *Biochem J* **126**, 1181–1191 (1972).

14. Stüven, R., Vollmer, M. & Bock, E. The impact of organic matter on nitric oxide formation by Nitrosomonas europaea. *Arch. Microbiol.* **158**, 439–443 (1992).

15. Yu, R., Perez-Garcia, O., Lu, H. & Chandran, K. *Nitrosomonas europaea* adaptation to anoxic-oxic cycling: Insights from transcription analysis, proteomics and metabolic network modeling. *Science of The Total Environment* **615**, 1566–1573 (2018).

16. Schreiber, F., Wunderlin, P., Udert, K. M. & Wells, G. F. Nitric oxide and nitrous oxide turnover in natural and engineered microbial communities: biological pathways, chemical reactions, and novel technologies. *Front Microbiol* **3**, 372 (2012).

17. Wunderlin, P., Mohn, J., Joss, A., Emmenegger, L. & Siegrist, H. Mechanisms of N2O production in biological wastewater treatment under nitrifying and denitrifying conditions. *Water Research* **46**, 1027–1037 (2012).

18. Lu, H. & Chandran, K. Factors promoting emissions of nitrous oxide and nitric oxide from denitrifying sequencing batch reactors operated with methanol and ethanol as electron donors. *Biotechnology and Bioengineering* **106**, 390–398 (2010).

19. US EPA, O. Effluent Guidelines. https://www.epa.gov/eg (2014).

20. Daelman, M. R. J., van Voorthuizen, E. M., van Dongen, U. G. J. M., Volcke, E. I. P. & van Loosdrecht, M. C. M. Seasonal and diurnal variability of N2O emissions from a full-scale municipal wastewater treatment plant. *Science of the Total Environment* **536**, 1–11 (2015).

21. Gernaey, K. V., van Loosdrecht, M. C. M., Henze, M., Lind, M. & Jørgensen, S. B. Activated sludge wastewater treatment plant modelling and simulation: state of the art. *Environmental Modelling & Software* **19**, 763–783 (2004).

22. Perez-Garcia, O., Mankelow, C., Chandran, K., Villas-Boas, S. G. & Singhal, N. Modulation of Nitrous Oxide (N2O) Accumulation by Primary Metabolites in Denitrifying Cultures Adapting to Changes in Environmental C and N. *Environ. Sci. Technol.* **51**, 13678–13688 (2017).

23. Frontiers | Metabolic Network Modeling of Microbial Interactions in Natural and Engineered Environmental Systems. https://www.frontiersin.org/journals/microbiology/articles/10.3389/fmicb.2016.00673/full.

24. Perez-Garcia, O., Chandran, K., Villas-Boas, S. G. & Singhal, N. Assessment of nitric oxide (NO) redox reactions contribution to nitrous oxide (N2O) formation during nitrification using a multispecies metabolic network model. *Biotechnology and Bioengineering* **113**, 1124–1136 (2016).

25. Perez-Garcia, O., Villas-Boas, S. G., Swift, S., Chandran, K. & Singhal, N. Clarifying the regulation of NO/N2O production in *Nitrosomonas europaea* during anoxic–oxic transition via flux balance analysis of a metabolic network model. *Water Research* **60**, 267–277 (2014).

26. Behera, C. R., Srinivasan, B., Chandran, K. & Venkatasubramanian, V. Model based predictive control for energy efficient biological nitrification process with minimal nitrous oxide production. *Chemical Engineering Journal* **268**, 300–310 (2015).

27. Khalil, M., AlSayed, A., Liu, Y. & Vanrolleghem, P. A. Machine learning for modeling N2O emissions from wastewater treatment plants: Aligning model performance, complexity, and interpretability. *Water Research* **245**, 120667 (2023).

28. Bellandi, G., Weijers, S., Gori, R. & Nopens, I. Towards an online mitigation strategy for N2O emissions through principal components analysis and clustering techniques. *J Environ Manage* **261**, 110219 (2020).

29. Villez, K. *et al.* Combining multiway principal component analysis (MPCA) and clustering for efficient data mining of historical data sets of SBR processes. *Water Sci Technol* **57**, 1659–1666 (2008).

30. Sobczyk, M., Pajdak-Stós, A., Fiałkowska, E., Sobczyk, Ł. & Fyda, J. Multivariate analysis of activated sludge community in full-scale wastewater treatment plants. *Environ Sci Pollut Res* **28**, 3579–3589 (2021).

31. Cui, F. *et al.* Application of principal component analysis (PCA) to the assessment of parameter correlations in the partial-nitrification process using aerobic granular sludge. *Journal of Environmental Management* **288**, 112408 (2021).

32. Çimen Mesutoğlu, Ö. & Gök, O. Prediction of COD in industrial wastewater treatment plant using an artificial neural network. *Sci Rep* **14**, 13750 (2024).

33. Liu, T., Zhang, H., Wu, J., Liu, W. & Fang, Y. Wastewater treatment process enhancement based on multi-objective optimization and interpretable machine learning. *Journal of Environmental Management* **364**, 121430 (2024).

34. Mathur, R. *et al.* Modeling of two-stage anaerobic onsite wastewater sanitation system to predict effluent soluble chemical oxygen demand through machine learning. *Sci Rep* **14**, 1835 (2024).

35. Zhang, Y. *et al.* Machine learning modeling for the prediction of phosphorus and nitrogen removal efficiency and screening of crucial microorganisms in wastewater treatment plants. *Science of The Total Environment* **907**, 167730 (2024).

36. Sheik, A. G. *et al.* Prediction of wastewater quality parameters using adaptive and machine learning models: A South African case study. *Journal of Water Process Engineering* **67**, 106185 (2024).

37. Seshan, S., Poinapen, J., Zandvoort, M. H., van Lier, J. B. & Kapelan, Z. Forecasting nitrous oxide emissions from a full-scale wastewater treatment plant using LSTM-based deep learning models. *Water Research* **268**, 122754 (2025).

38. Xu, X. *et al.* Prediction of nitrous oxide emission of a municipal wastewater treatment plant using LSTM-based deep learning models. *Environ Sci Pollut Res* **31**, 2167–2186 (2024).

39. Li, K. *et al.* An Integrated First Principal and Deep Learning Approach for Modeling Nitrous Oxide Emissions from Wastewater Treatment Plants. *Environmental Science and Technology* **56**, 2816–2826 (2022).

40. Khalil, M., AlSayed, A., Liu, Y. & Vanrolleghem, P. A. An integrated feature selection and hyperparameter optimization algorithm for balanced machine learning models predicting N2O emissions from wastewater treatment plants. *Journal of Water Process Engineering* **63**, 105512 (2024).

41. Ahn, J. H., Kwan, T. & Chandran, K. Comparison of Partial and Full Nitrification Processes Applied for Treating High-Strength Nitrogen Wastewaters: Microbial Ecology through Nitrous Oxide Production. *Environ. Sci. Technol.* **45**, 2734–2740 (2011).

42. Kim, Y. M., Park, H. & Chandran, K. Nitrification inhibition by hexavalent chromium Cr(VI)--Microbial ecology, gene expression and off-gas emissions. *Water Res* **92**, 254–261 (2016).

43. Brotto, A. C., Annavajhala, M. K. & Chandran, K. Metatranscriptomic Investigation of Adaptation in NO and N2O Production From a Lab-Scale Nitrification Process Upon Repeated Exposure to Anoxic–Aerobic Cycling. *Front Microbiol* **9**, 3012 (2018).

44. Li, B. & Wu, G. Effects of Sludge Retention Times on Nutrient Removal and Nitrous Oxide Emission in Biological Nutrient Removal Processes. *Int J Environ Res Public Health* **11**, 3553–3569 (2014).

45. Brotto, A. C. *et al.* Factors controlling nitrous oxide emissions from a full-scale activated sludge system in the tropics. *Environ Sci Pollut Res* **22**, 11840–11849 (2015).

46. Wang, A.-J. *et al.* Digital Twins for Wastewater Treatment: A Technical Review. *Engineering* **36**, 21–35 (2024).

47. Zhou, J. *et al.* Sub-period division strategies combined with multiway principle component analysis for fault diagnosis on sequence batch reactor of wastewater treatment process in paper mill. *Process Safety and Environmental Protection* **146**, 9–19 (2021).

48. AL-Kordy, S. U. & Khudair, D. B. H. Effluent quality assessment of sewage treatment plant using principal component analysis and cluster analysis. *Journal of Engineering* **27**, 79–95 (2021).

49. Liu, H., Yang, J., Zhang, Y. & Yang, C. Monitoring of wastewater treatment processes using dynamic concurrent kernel partial least squares. *Process Safety and Environmental Protection* **147**, 274–282 (2021).

50. Yang, C., Zhang, Y., Huang, M. & Liu, H. Adaptive dynamic prediction of effluent quality in wastewater treatment processes using partial least squares embedded with relevance vector machine. *Journal of Cleaner Production* **314**, 128076 (2021).

51. Chandran, K., Pagilla, K. & Katehis, D. Field Protocol With Quality Assurance Plan - Characterization of Nitrogen Greenhouse Gas Emissions From Wastewater Treatment Bnr Operations. 1–47 (2009).

52. Chandran, K. *Protocol for the Measurement of Nitrous Oxide Fluxes from Biological Wastewater Treatment Plants*. *Methods in Enzymology* vol. 486 (Elsevier Inc., 2011).

53. Gruber, W. *et al.* Estimation of countrywide N2O emissions from wastewater treatment in Switzerland using long-term monitoring data. *Water Research X* **13**, (2021).

54. Andrew D. Eaton, American Water Works Association, Water Environment Federation. *Standard Methods for the Examination of Water and Wastewater*. (APHA-AWWA-WEF, Washington, D.C., 2005).

55. Stekhoven, D. J. & Bühlmann, P. MissForest—non-parametric missing value imputation for mixed-type data. *Bioinformatics* **28**, 112–118 (2012).

Tables and Figures

Table 1. Summary of N_2O emission factor at a mainstream and sidestream process configuration in a Full-Scale BNR WWTPs

629

Plant configuration	Temp (°C)	Q (MGD)	Influent TKN load (g-N/day)	Removed TN load (g-N/day)	% Nitrogen removed	% influent TKN emitted as N_2O (EF)	Ref
Step feed BNR	18±3	21	1.6E+06	1.0E+06	62±21	0.20±0.03	This study
	23±3	23	1.6E+06	8.5E+05	56±16	0.03±0.006	
PdNA	18±1.7	15	1.8E+06	1.2E+06	68±7	0.006±0.00	
	25±2.8	12	2.1E+06	1.7E+06	77±8	0.005±0.00	
ABAC	26±2.2	23	1.4E+06	NA	NA	0.004±0.00	
Fermentate-fed denitrification	25±0.7	2.0	4.7E+01	3.3E+01	71±20	0.003±0.00	
SHARON	30±0.56	0.88	2.24E+06	8.28E+05	37±16	8.0±3.4	
Separate-stage BNR	15±0.48	23	1.8E+06	3.6E+05	20±1	0.03±0.00	Ahn. et al[4]
	23±0.28	27	2.3E+06	4.3E+05	19±4	0.01±0.00	
Four-stage Bardenpho	14±0.26	7.8	8.6E+05	1.7E+05	20±1	0.16±0.10	
	23±0.20	8.1	7.4E+05	7.6E+04	10±4	0.60±0.29	
Step-feed BNR 1	19±0.22	29	3.1E+06	1.4E+06	45±8	1.6±0.83	
	25±0.28	30	2.9E+06	9.4E+05	32±10	0.62±0.27	
Step-feed non-BNR	17±0.12	71	8.6E+06	4.4E+06	51	0.18±0.18	
	26±0.81	93	8.9E+06	4.2E+06	47	1.8±0.79	
Separate centrate	30±2.3	2.0	8.8E+06	5.5E+06	63	0.24±0.02	
	34±0.32	1.6	8.5E+06	4.2E+06	49	0.54±0.16	
Plug-flow 1	11±0.20	18	1.8E+06	1.0E+06	56	0.40±0.14	
	23±0.46	15	1.8E+06	7.3E+05	41	0.41±0.14	
Plug-flow 2	11±0.41	8.7	6.3E+05	4.0E+05	63	0.62±0.15	
	22±0.58	6.6	6.6E+05	4.0E+05	61	0.09±0.03	
MLE 1	26±1.8	4.0	6.8E+05	1.9E+05	28	0.07±0.04	
MLE 2	26±0.17	4.1	6.9E+05	1.5E+05	22	0.06±0.02	
Step-feed BNR 2	29±0.18	14	2.2E+06	2.9E+05	13	1.5±0.02	
Oxidation ditch	19±0.58	3.4	3.9E+05	4.3E+04	11±1	0.03±0.01	
Step-feed BNR 3	24±0.78	57	7.8E+06	8.6E+05	11±2	0.05±0.03	

Legend of Figures

Figure 1. PCA analysis on N_2O flux and wastewater quality parameters. A,B, Multivariate relationships between N_2O flux (g-N min^{-1}-m^2) and local versus global variables in aerobic **(A)** and anoxic **(B)** zones. Blue arrows indicate variable loadings and their directionality along principal components, reflecting contributions to N_2O flux. The analysis included 1439 samples, with principal components 1 and 2 shown as they captured the greatest variance.

Figure 2. Data collection and processing in ML with variable importance score from the XG Boost algorithm. A, Workflow integrating real-time N_2O emission data, N-profile and plant operational data, into ML models to identify mitigation strategies to reduce N_2O emissions and improve water-sanitation system. **B,C,** permutation importance scores showing contribution of individual variables to predicted N_2O flux in aerobic **(B)** and anoxic **(C)** zones.

Figure 3. SHAP analysis of predicted N_2O flux across wastewater parameters. A,B, Beeswarm plots showing the magnitude and direction of variable contributions to predicted N_2O flux in aerobic **(A)** and anoxic **(B)** zones. The feature values are normalized to highlight variability and the influence of local and global parameters on N_2O flux.

Figure 4. PDP on predicted N_2O flux with selective key features. Two-dimensional PDP showing predicted N_2O flux and its dynamic relationship towards key process variables in aerobic **(A,B)** and anoxic **(C,D)** zones. Predicted N_2O flux with **(A)** NH_3 and SRT, **(B)** NH_3 and DO, **(C)** DO and SRT, **(D)** DO and NO_2^-.

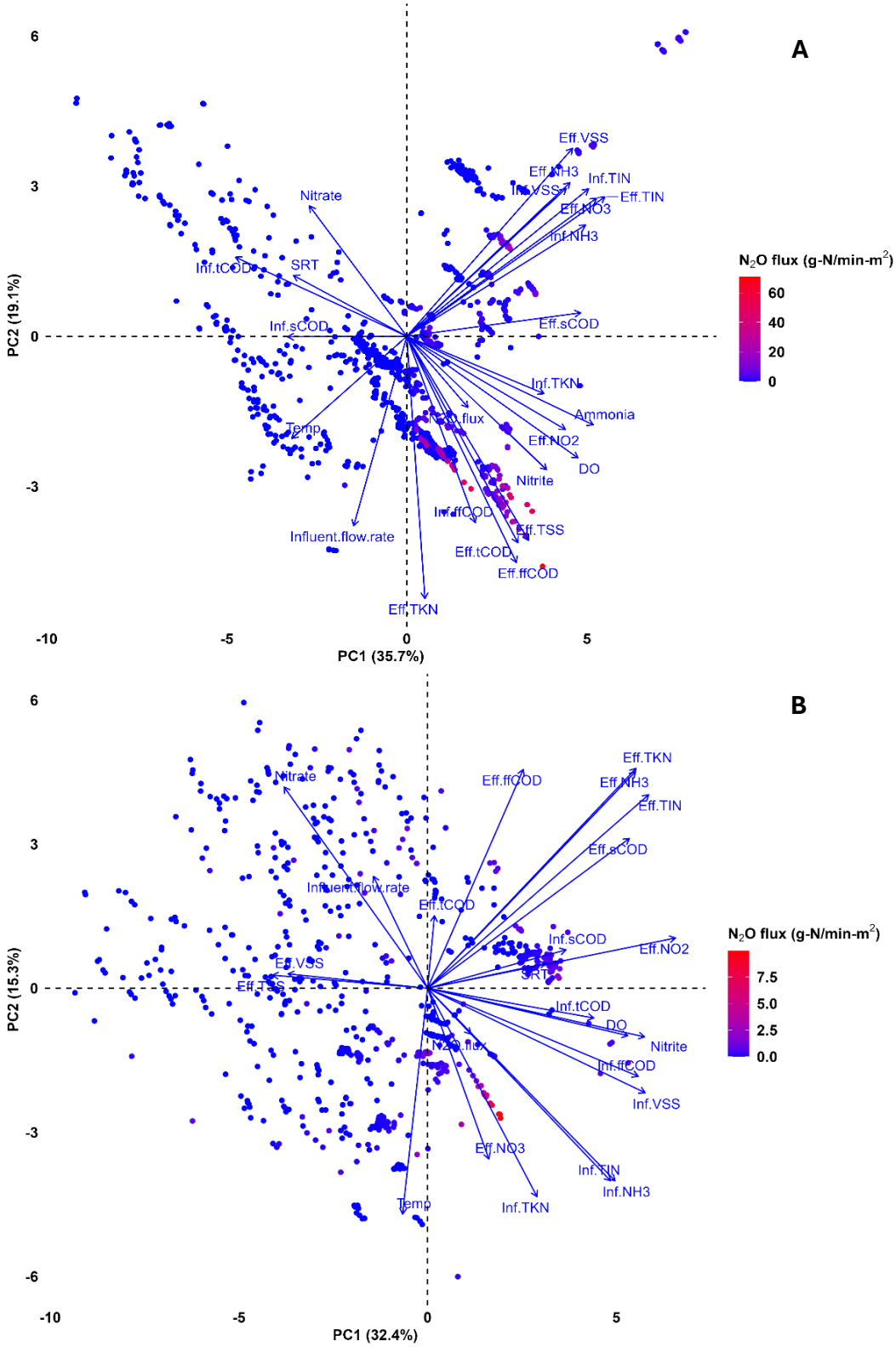

Figure 1. PCA analysis on N_2O flux and wastewater quality parameters. A,B, Multivariate relationships between N_2O flux (g-N min^{-1}-m^2) and local versus global variables in aerobic **(A)** and anoxic **(B)** zones. Blue arrows indicate variable loadings and their directionality along principal components, reflecting contributions to N_2O flux.

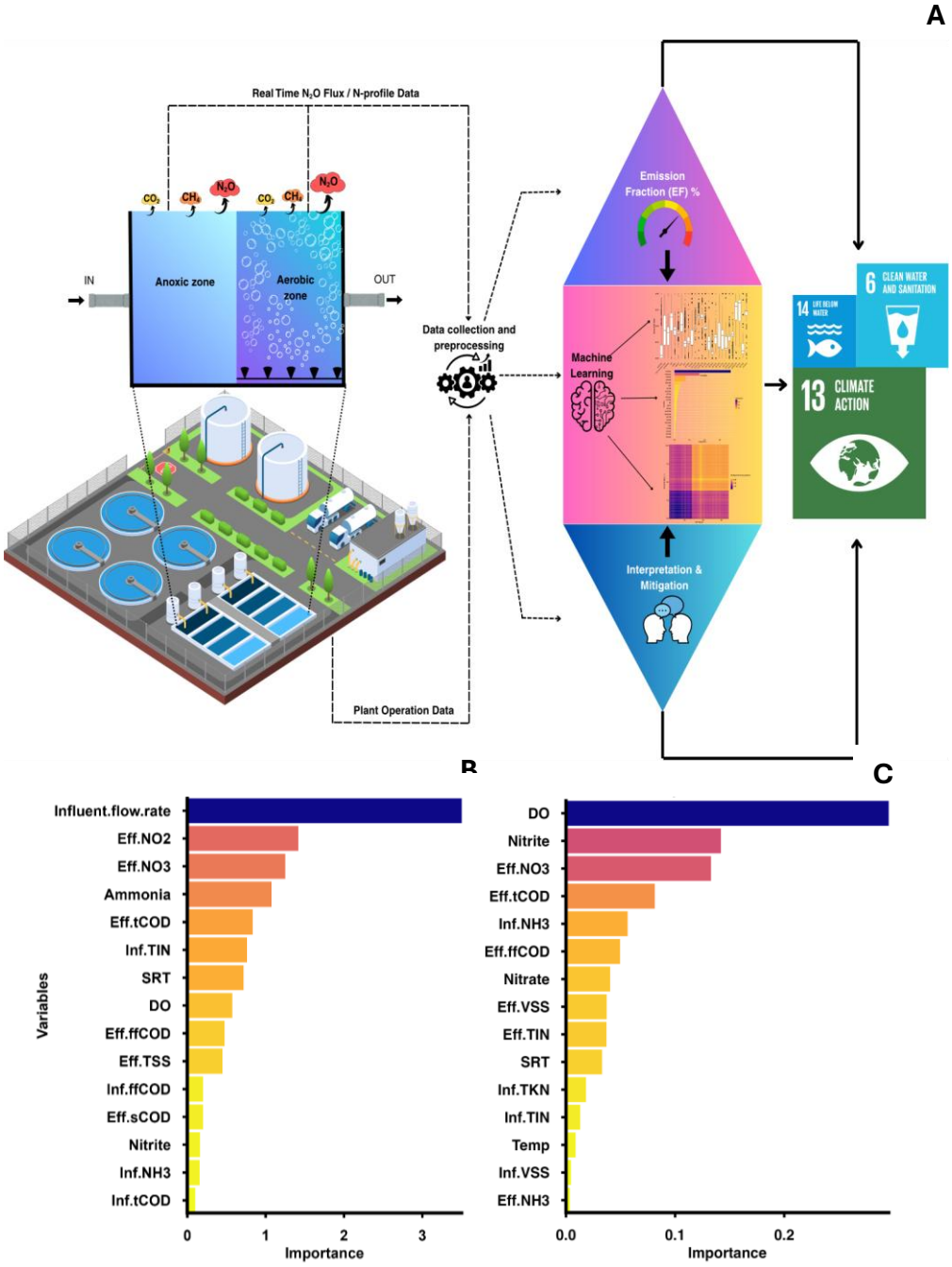

Figure 2. Data collection and processing in ML with variable importance from the XG Boost algorithm. A, workflow integrating real-time N_2O emission data, N-profile and plant operational data, into ML models to identify mitigation strategies to reduce N_2O emissions and improve the water-sanitation system. **B,C,** XG boost permutation importance scores showing contribution of individual variables to predicted N_2O flux in aerobic **(B)** and anoxic **(C)** zones.

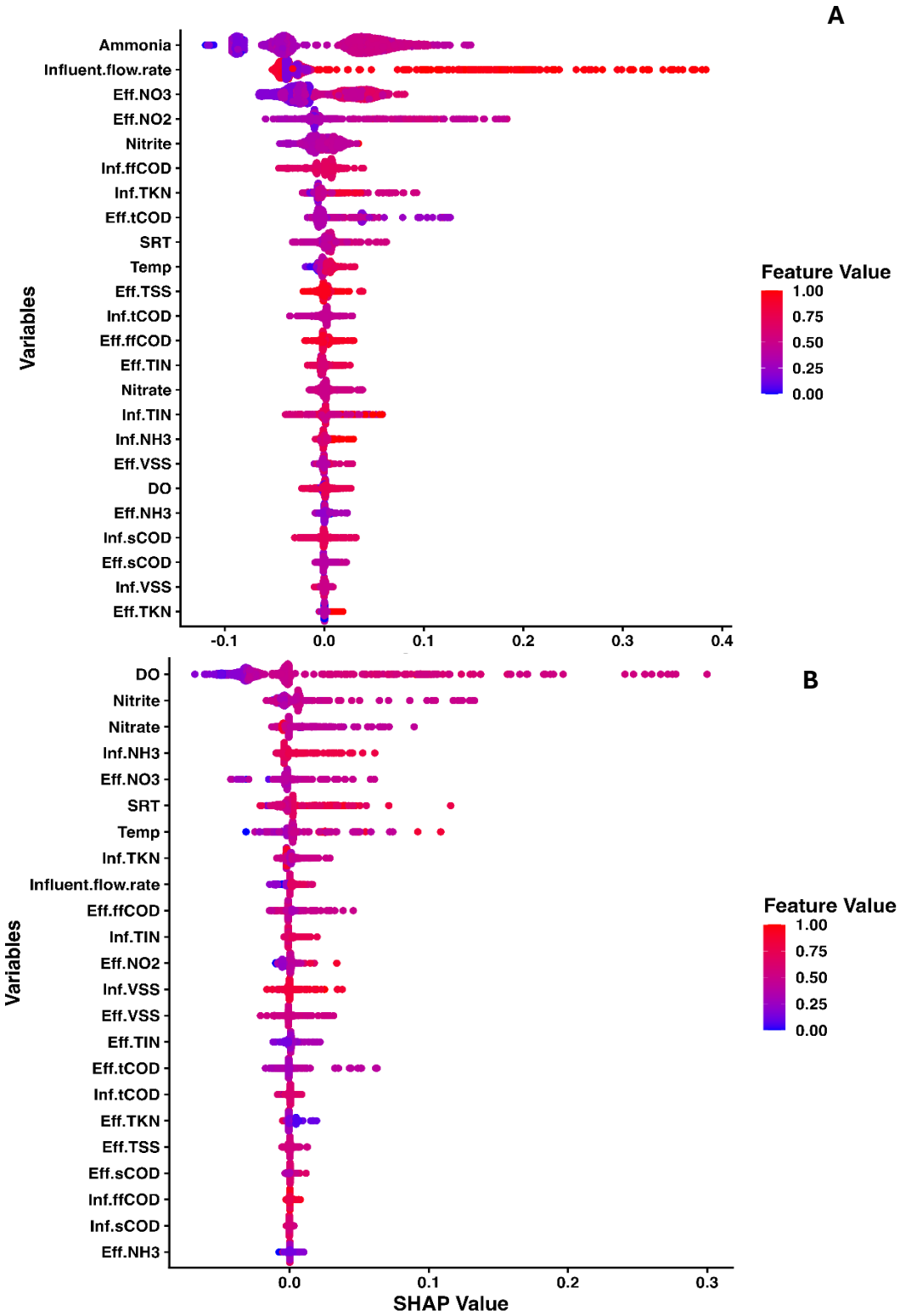

Figure 3. SHAP analysis of predicted N_2O flux across wastewater parameters. A,B, Beeswarm plots showing the magnitude and direction of variable contributions to predicted N_2O flux in aerobic **(A)** and anoxic **(B)** zones. The feature values are normalized to highlight variability and the influence of local and global parameters on N_2O flux.

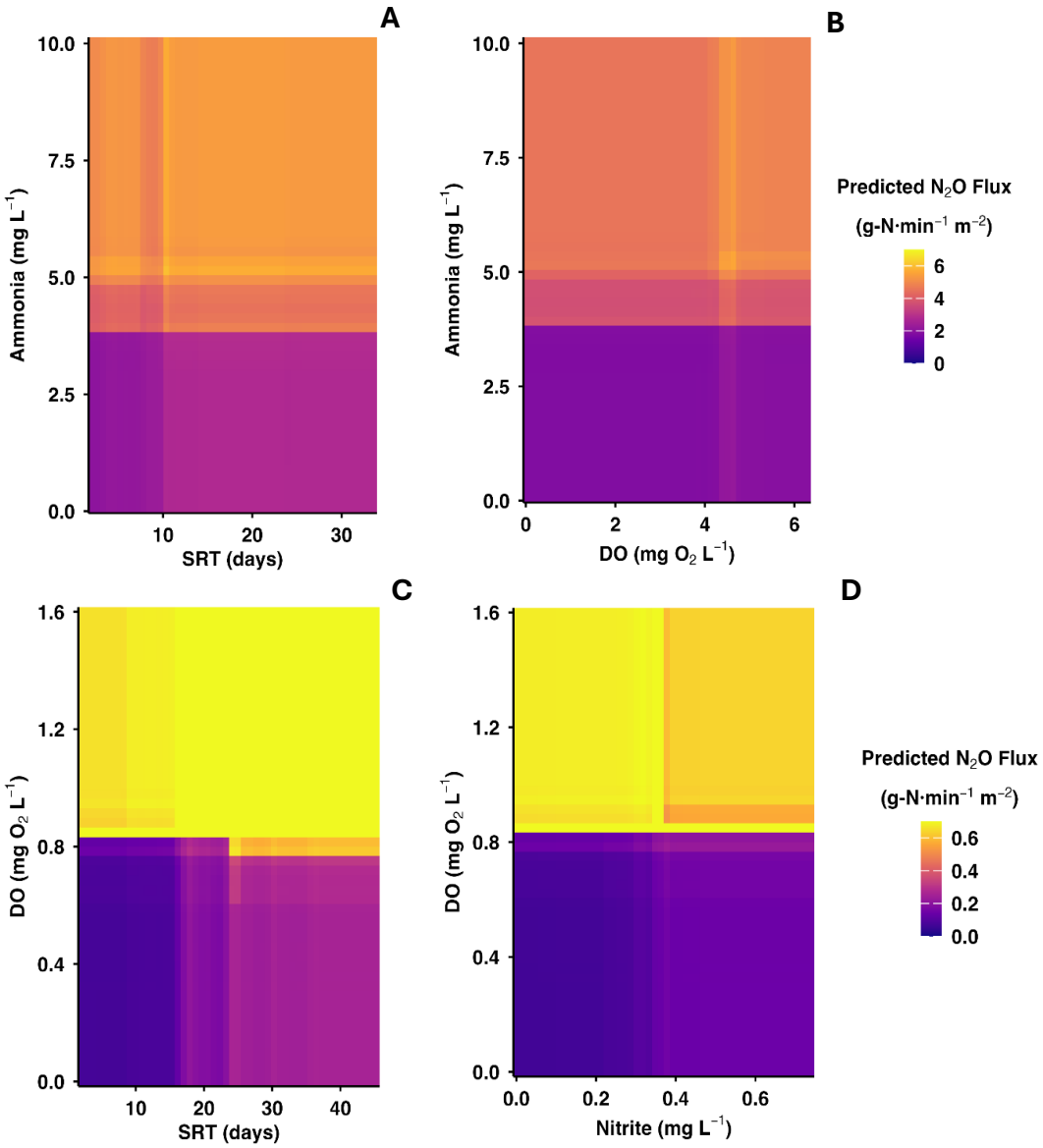

Figure 4. PDP on predicted N_2O flux with selective key features. Two-dimensional PDP showing predicted N_2O flux and its dynamic relationship towards key process variables in aerobic **(A,B)** and anoxic **(C,D)** zones. Predicted N_2O flux with **(A)** NH_3 and SRT, **(B)** NH_3 and DO, **(C)** DO and SRT, **(D)** DO and NO_2^-.